Sestrin-2 regulates podocyte mitochondrial dysfunction and apoptosis under high-glucose conditions via AMPK

QIAOXUAN LIN, YIQIONG MA, ZHAOWEI CHEN, JIJIA HU, CHENG CHEN, YANQIN FAN, WEI LIANG and GUOHUA DING

Department of Nephrology, Renmin Hospital of Wuhan University, Wuhan, Hubei 430060, P.R. China

Received September 26, 2019; Accepted January 28, 2020

DOI: 10.3892/ijmm.2020.4508

Abstract. Diabetic kidney disease (DKD) is a severe form of microangiopathy among diabetic patients, of which podocyte injury is one of the more predominant features. There is increasing evidence to suggest that mitochondrial dysfunction is associated with podocyte injury, thus contributing to the progression of DKD. Initially identified as a p53 target protein, the endogenous antioxidant protein, sestrin-2 (sesn2), has recently attracted attention due to its potential function in various inflammatory diseases. However, the association between sesn2 and podocytes in DKD remains unclear. In the present study, to elucidate the role of sesn2 in podocyte mitochondrial dysfunction, the effects of sesn2 on the regulation of AMP-activated protein kinase (AMPK) were examined *in vitro* and *in vivo*. Abnormal mitochondria were found in rats with streptozotocin-induced diabetes, and hyperglycemia downregulated the expression of sesn2. The upregulation of sesn2 increased the level of AMPK phosphorylation, and thus ameliorated mitochondrial dysfunction under high glucose conditions (HG). On the whole, these results suggest that sesn2 is associated with mitochondrial dysfunction in podocytes under HG conditions. In addition, the decreased expression of sesn2 may be a therapeutic target for DKD.

Introduction

As one of the most common and severe microvascular complications among patients with diabetes mellitus, diabetic kidney disease (DKD) impairs renal function and leads to end-stage renal disease (ESRD) (1). Associated with higher mortality and morbidity, the disease poses a substantial financial and healthcare burden worldwide. The primary pathological changes associated with DKD include glomerular cell hypertrophy, podocyte depletion and the thickening of the glomerular basement membrane, which results in increased urinary protein levels (2). By synthesizing extracellular matrix and cytoskeletal proteins, podocytes play an indispensable role in glomerular filtration, and as a result, are rich in mitochondria (3). Over the years, an increasing numbers of studies have indicated that perturbed mitochondrial function contributes to the pathogenesis of DKD (4-6), as the mitochondria are involved in various cellular functions, including oxidative damage and apoptosis. Hence, it has been hypothesized that the identification of key molecules involved in podocyte mitochondrial dysfunction may be a promising therapeutic strategy for patients with DKD.

As members of the highly-conserved family of stress-responsive proteins with antioxidant properties, sestrins exist in three mammalian isoforms, sestrin-1 (sesn1), sesn2 and sesn3, while invertebrates have only one form (7,8). Two important functions of sestrins are to suppress the formation of reactive oxygen species (ROS) (9) and to inhibit the activity of mammalian target of rapamycin complex 1 (mTORC1) (10). The ROS-suppressive function of sesn2 is partly dependent on the inhibition of mTORC1, which increases the degradation of damaged mitochondria or on the nuclear factor erythroid 2-related factor 2 (Nrf2)-inhibitor, Keap1 (11-13). When exposed to environmental and metabolic stress (such as DNA damage, oxidative stress, endoplasmic reticulum stress, hypoxia, energy deprivation and amino acid starvation), sesn2 begins to accumulate, thus protecting cells from damage (8,9,14). Considering these important findings, sesn2 has been hypothesized to protect podocytes by maintaining mitochondrial homeostasis under high glucose (HG) conditions.

Interactions between sesn2 and the AMP-activated protein kinase (AMPK) pathway have been reported to play an important role in the regulation of energy homeostasis, cellular proliferation and apoptosis (15,16). As a member of the serine-threonine protein kinase family, AMPK is an essential energy sensor which maintains cellular and whole-body energy homeostasis. There is also increasing evidence to indicate the potential antioxidant properties of AMPK, and its role in the preservation of mitochondrial function (2). Experiments conducted with streptozotocin (STZ)-induced diabetic mice have revealed that renal damage is alleviated by improving mitochondrial function with an AMPK agonist (17). In the

Correspondence to: Professor Guohua Ding, Department of Nephrology, Renmin Hospital of Wuhan University, 238 Jiefang Road, Wuhan, Hubei 430060, P.R. China
E-mail: ghxding@qq.com

Key words: sestrin-2, podocytes, diabetic kidney disease, mitochondrial dysfunction, AMP-activated protein kinase

present study, it was hypothesized that sesn2 may ameliorate mitochondrial dysfunction via the activation of the AMPK pathway.

Therefore, the aim of the present study was to determine whether the antioxidant effects of sesn2 were active against HG conditions, which was achieved by analyzing the expression levels of sesn2 in human podocytes following treatment with HG (to mimic diabetic conditions) and in diabetic rats, respectively. The molecular role of sesn2 in mitochondria and AMPK signaling was also investigated.

Materials and methods

Human renal biopsy samples. Six renal biopsy samples (3 from males and 3 from females; age, 40-66 years; mean age, 53.5±8.71 years) from patients diagnosed with DKD were obtained from the Division of Nephrology, Renmin Hospital of Wuhan University (Wuhan, China). Six control samples (3 from males and 3 from females; age, 37-67 years; mean age, 51.0±9.59 years) were para-carcinoma tissues from patients without diabetes who underwent tumor nephrectomies, and were obtained from the Division of Pathology (Renmin Hospital of Wuhan University); biochemical analysis (urine albumin-to-creatinine ratio <30 mg/g) and histological examination revealed no features of DKD apart from solitary renal cell carcinoma. Investigations were based on the principles of the Declaration of Helsinki (18). Experiments were performed according to the approved guidelines of Wuhan University and were approved by the Research Ethics Committee of Renmin Hospital of Wuhan University after written informed consent was received from the patients.

Animals. All animal experiments conformed to the Regulations of Animal Experiments in Wuhan University, and were approved by the Ethical Committee for the Experimental Use of Animals at Renmin Hospital of Wuhan University. Both the diabetic and control rats were maintained as previously described (19). A total of 12 8-week-old male SD rats were housed in cages and raised in an environment with a temperature of 21-23˚C (55±10% humidity). The rats were randomly allocated to the control (6 rats) and diabetic groups (6 rats) and they were provided with free access to food and sterile water throughout the experiment. Diatetes was induced by an intraperitoneal injection of STZ (80 mg/kg; Sigma-Aldrich; Merck KGaA) dissolved in 0.1 M citrate buffer (pH 4.5) 5 times daily. The control rats received citrate buffer alone. Urine and blood glucose were measured regularly; the rats were considered diabetic when glycemic levels exceeded 200 mg/dl 1 week after the final STZ (80 mg/kg; Sigma-Aldrich; Merck KGaA) intraperitoneal injection, and when glycosuria was detectable (Uristix; Ames DVN) within 36 h. Blood was obtained from the tail vein and assayed using a blood glucose analyzer (Contour® TS; Bayer). After 12 weeks of diabetes, urine at 24 h was collected in metabolic cages, and urinary albumin concentrations were determined. Kidney samples were collected under anesthesia by an intraperitoneal injection using 10% chloral hydrate at a dose of 300 mg/kg. Depth of anesthesia was assessed (heart rate, respiration frequency, temperature, righting reflex, corneal reflex and pupillary light reflex) and peritonitis or other adverse reactions were not observed throughout the experiments. The kidneys were fixed in 10% formaldehyde and then embedded in paraffin (for histological evaluation) or OCT compound (Sakura Finetek Europe B.V.), and stored at -80˚C.

Isolation of glomeruli. The renal glomeruli were isolated by a sieving method. The rats were sacrificed by cervical dislocation under anesthesia by an intraperitoneal injection using 10% chloral hydrate at a dose of 300 mg/kg and the kidneys were harvested. Kidneys from rats were minced into 1 mm^3 sections on ice and digested in Glomeruli Digest solution which consists of Worthington Collagenase II, Pronase E and DNase at 37˚C. The digest was filtered using a cell strainer (100-70-40 μm mesh openings) on the 50 ml tube subsequently, which was washed by the complete Hanks' buffered salt solution at the same time. A new 50 ml Falcon was used to harvest glomeruli from the inner layer of the strainer (40 μm) with complete HBSS. The glomeruli-containing solution was centrifuged at 1,500 x g at 4˚C for 5 min and the supernatant was discarded.

Cells and cell culture. Conditionally immortalized human podocytes were kindly provided by Dr Moin A. Saleem (Academic Renal Unit, Southmead Hospital, Bristol, UK) and cultured at 33˚C in RPMI-1640 medium (HyClone; GE Healthcare Life Sciences) with 10% fetal bovine serum (Gibco; Thermo Fisher Scientific, Inc.), 100 ml streptomycin, 100 U/ml penicillin G and 1X insulin-transferrin-selenium (ITS; both Thermo Fisher Scientific, Inc.) for proliferation. For differentiation, the podocytes were transferred to an incubator at 37˚C and cultured in ITS-free medium for 7-14 days. For synchronization, the podocytes were starved in serum-free medium for 12 h. For HG stimulation, the cells were cultured in normal glucose (5 mM), HG (35 mM) or hypertonic solution (5 mM glucose combined with 30 mM mannitol). The D-glucose and mannitol were purchased from Sigma-Aldrich (Merck KGaA). The AMPK activator, aminoimidazole carboxamide ribonucleotide (AICAR, 2 mM, 12 h), was purchased from Sigma-Aldrich (Merck KGaA), and the AMPK inhibitor, compound C (C.C, 0.1 mM, 2 h), was purchased from MedChemExpress. All results were performed using ≥3 independent podocyte cultures.

Transfection. sesn2-siRNA was purchased from Shanghai GenePharma Co., Ltd., and transfection was performed using the HiPerFect Transfection Reagent according to the manufacturer's protocol (Qiagen GmbH). A total of $2x10^5$ cells were seeded into six6well plates and transfected with sesn2-siRNA or a negative control scramble siRNA (Shanghai GenePharma Co., Ltd.). The siRNA sequence was as follows: SESN2-homo-1650, 5'-GCGGAACCUCAAGGUCUAUTT-3'.

To upregulate the expression of sesn2, a sesn2 overexpression plasmid was purchased from Shanghai Genechem Co., Ltd. and transfected into the cells using X-tremeGENETM Transfection Reagent (Roche Diagnostics) according to the instructions provided by the manufacturer.

Western blot analysis. Podocytes and glomeruli were lysed on ice in radio immunoprecipitation assay buffer (Beyotime Institute of Biotechnology) supplemented with

protease/phosphatase inhibitor cocktail (Sigma-Aldrich; Merck KGaA) and PMSF (Beyotime Institute of Biotechnology). The lysates were centrifuged at 12,000 x g at 4˚C for 10 min, and the supernatants were subsequently mixed with 5X loading buffer before being boiled at 100˚C for 5 min. The total protein concentrations were determined using a BCA protein assay (Thermo Fisher Scientific, Inc.). Equal amounts of 10 μl protein were separated by 10% SDS-PAGE and then electro-transferred onto PVDF membranes (EMD Millipore). After blocking with 5% skimmed milk for 1-2 h at room temperature, the membranes were incubated with primary antibodies [sesn2 rabbit monoclonal antibody, 1:1,000, ab178518, Abcam; p-AMPKα1/2 (Thr172) rabbit polyclonal antibody, 1:100, #2535, Cell Signaling Technology; AMPKα1/2 (H-300) rabbit polyclonal antibody, 1:100, sc-74461, Santa Cruz Biotechnology, Inc.; and GAPDH mouse monoclonal antibody, 1: 1,000, ANT011, Antgene] overnight at 4˚C. Alexa Fluor 680/790-labeled goat anti-rabbit/goat anti-mouse IgG (1:10,000, P/N 926-65020, LI-COR Biosciences) was used as the secondary antibody at 37˚C for 1 h and the blots were visualized using an Odyssey Infrared Imaging System (LI-COR Biotechnology). For quantification, the protein bands were analyzed with ImageJ software V1.8.0 (National Institutes of Health).

Immunofluorescence assay. Following fixation with 4% paraformaldehyde for 30 min and permeabilization in 0.2% Triton X-100 (PBS) at 4˚C, the frozen kidney sections were blocked with 5% bovine serum albumin (Antgene) at room temperature for 1 h. The sections were then incubated with a mixture of primary antibodies against sesn2 rabbit monoclonal antibody (1:100; ab178518, Abcam) and mouse anti-snaptopodin (1:200; sc-515842, Santa Cruz Biotechnology, Inc.) overnight at 4˚C. The sections were subsequently stained with a mixture of Alexa Fluor 488, donkey anti-rabbit IgG (HL) (1:200; ANT024s, Antgene) and Alexa Fluor 594, donkey anti-Mouse IgG (HL) (1:200; ANT029s, Antgene) secondary antibodies at 37˚C for 60 min in the dark. The nuclei were counterstained with DAPI (Antgene) at 37˚C for 5 min.

The cell climbing films were fixed in 4% paraformaldehyde for 20 min at 4˚C, and blocked with 5% bovine serum albumin (Antgene) at room temperature for 1 h. The films were then stained with the following antibodies at 4˚C overnight: Sesn2 rabbit monoclonal antibody (1:100; ab178518, Abcam). The films were then incubated with Alex Fluor 488, donkey anti-rabbit IgG (HL) (1:200; ANT024s, Antgene) at 37˚C for 60 min in the dark. The nuclei were counterstained with DAPI 37˚C for 5 min. All microscopic images were visualized with a fluorescence microscope (Olympus Corp.).

Apoptosis assay. Flow cytometry was performed to assess the degree of podocyte apoptosis *in vitro*; double staining was conducted using the Annexin V-PE-7AAD Apoptosis Detection kit I (BD Biosciences) according to the manufacturer's instructions. Samples were analyzed on a BD Accuri C6 flow cytometer (BD Biosciences) and cells in the upper- and lower-right quadrants were classified as apoptotic.

Assessment of mitochondrial membrane potential (MMP). To evaluate MMP, JC-1 staining was conducted using the Mitochondrial membrane potential assay kit with JC-1 (Beyotime Institute of Biotechnology) as per the manufacturer's instructions. Images were captured with a fluorescence microscope (Olympus Corp.), where green fluorescence indicated the J-monomer and red fluorescence indicated the J-aggregate. The images were analyzed using ImageJ software V1.8.0 (National Institutes of Health).

Detection of ROS. The dichlorofluorescein diacetate (DCFH-DA; Beyotime Institute of Biotechnology) fluorescent probe was used to measure intracellular ROS levels. Cells were incubated with 10 μM DCFH-DA at 37˚C for 1 h, and then washed 3 times with PBS. Images were subsequently captured using a fluorescence microscope (Olympus Corp.).

Co-immunoprecipitation. The experiments were performed using a kit (Beyotime Institute of Biotechnology) according to the manufacturer's instructions. Total protein was extracted from the cultured podocytes using lysis buffer (20 mM Tris, 150 mM NaCl, 1.0% Triton X-100, 5 mM EDTA and 1 mM phenylmethylsulfonyl fluoride, pH 7.5). A sesn2 mouse monoclonal antibody (1:100; sc-393195, Santa Cruz Biotechnology) or IgG (1:100, #2729, Cell Signaling Technology) was added to the protein samples, which were then rotated overnight at 4˚C. Subsequently, the samples were mixed with 40 μl of protein A+G agarose and incubated for 3 h at 4˚C. The beads were mixed with 1X Lane Marker Sample Buffer. After being boiled at 100˚C for 5 min, the samples were processed for western blot analysis.

Transmission electron microscopy. To observe mitochondrial morphology, the rat kidneys were imaged by transmission electron microscopy. Kidney tissues were fixed in 2.5% glutaraldehyde (340855, Sigma-Aldrich). The dissected tissues were washed with PBS and post-fixed in 2% osmium tetroxide for 2 h at room temperature. The fixed tissues were dehydrated in a graded alcohol series and embedded in Epon. Following the polymerization of Epon, the blocks were sectioned to generate 70-nm-thick sections using a microtome (Leica). The sections were double-stained with uranyl acetate and lead citrate at room temperature for 2 h and finally examined and imaged with a 100CX JEOL transmission electron microscope (Hitachi).

Histopathological staining. Hematoxylin and eosin (H&E) staining and Periodic Acid-Schiff (PAS) staining were conducted to observe the histopathological changes. The samples from kidney were fixed with 4% paraformaldehyde, embedded in paraffin and sectioned at 2.5 μm. Briefly, following deparaffinization and rehydration, the sections were stained with hematoxylin solution for 5 min followed by 5 dips in 1% acid ethanol (1% HCl in 70% ethanol) and then rinsed in distilled water. The sections were then stained with eosin solution for 3 min and followed by dehydration with graded alcohol and clearing in xylene at room temperature. All chemical reagents were purchased from Beijing Sinopharm Chemical Reagents Co. Ltd.

Statistical analysis. All experiments were performed in duplicate and independently repeated at least 3 times. All data are

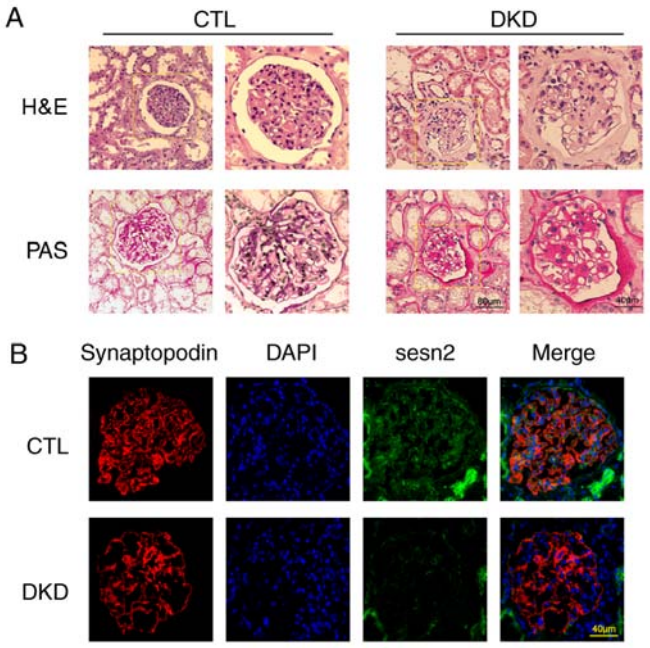

Figure 1. sesn2 expression in podocytes from patients with DKD. Patients were divided into 2 groups: i) the control (CTL), including patients without diabetes; and ii) the DKD group, including patients with diabetic kidney disease. (A) Representative micrographs of H&E-stained kidney sections and Periodic acid-Schiff-stained kidney sections of individuals from each group. (B) Representative images of immunofluorescent staining of synaptopodin, sesn2 and DAPI in the kidney sections of individuals from each group. sesn2, sestrin-2; DKD, diabetic kidney disease.

presented as the means ± SD, and analyzed using GraphPad Prism 8 (GraphPad Software, Inc.). Differences in the mean values were determined using the Student's t-test or one-way ANOVA followed by the LSD multiple comparison test. SPSS, version 22.0 (SPSS, Inc.), and $P<0.05$ was considered to indicate a statistically significant difference.

Results

sesn2 expression in podocytes from patients with DKD. HE and PAS staining were conducted for the initial diagnosis of patients with DKD, and the glomeruli of these patients exhibited pathological changes, including extracellular matrix deposition (Fig. 1A). According to the Human Protein Atlas (http://www.proteinatlas.org/) database, sesn2 is widely expressed in human renal glomeruli. In the present study, the triple immunofluorescent staining of sesn2, the podocyte marker synaptopodin and DAPI was performed to evaluate sesn2 expression in glomerular podocytes (Fig. 1B). sesn2 was predominantly localized in the cytoplasm of the podocytes. The results also revealed a decreased sesn2 expression in glomerular podocytes from subjects diagnosed with DKD, compared to those from healthy individuals, suggesting that this decrease may be associated with HG.

Histopathological features of glomeruli and podocyte injury from rats with STZ-induced diabetes. To verify the successful induction of diabetes, blood glucose levels, final body weight, albumin creatinine ratio (ACR) and urine total proteins (UTP) at 24 h were monitored (Table I). Compared with the control group, the diabetic rats exhibited higher blood glucose levels and a lower body weight; elevated levels of ACR and UTP in the diabetic rats also suggested an impaired renal function. The histological observations revealed typical features of DKD, including mesangial expansion from 12 weeks after modeling (Fig. 2A). Furthermore, transmission electron microscopy revealed obvious diffuse foot process fusion, indicating podocyte damage in diabetic rats (Fig. 2B).

Table I. Comparison of blood glucose, body weight, albumin creatinine ratio and urine total protein at 24 h between the controls (CTL) and rats with STZ-induced diabetes.

Parameters	CTL	STZ
Blood glucose (mmol/l)	7.14±0.16	32.36±1.33[a]
Final body weight (g)	579±33.25	368.47±22.95[a]
ACR (mg/g)	5.88±2.34	44.28±14.17[a]
UTP (mg)	9.12±2.66	51.36±6.35[a]

Rats were divided into 2 groups: i) the control (CTL), where rats received citrate buffer alone; and ii) STZ group, where rats received an intraperitoneal injection of streptozotocin; [a]$P<0.05$ vs. CTL (n=6 in each group).

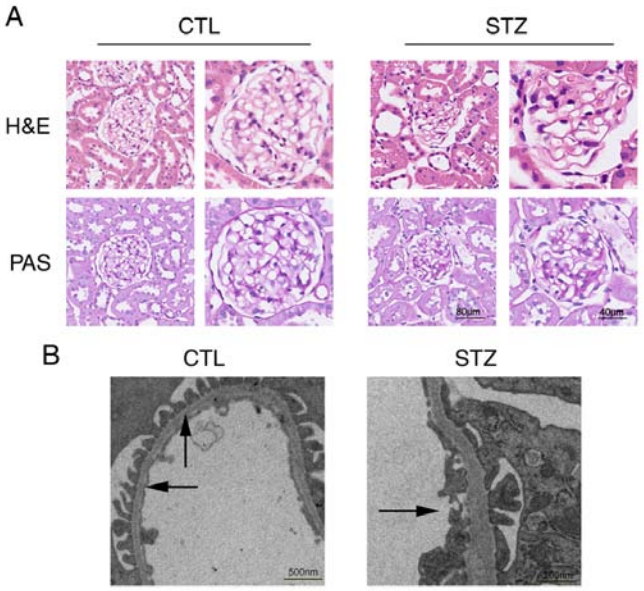

Figure 2. Histopathological features of glomeruli and podocyte injury from streptozotocin-induced diabetic rats. Rats were divided into 2 groups: i) the control (CTL), in which rats received citrate buffer alone; and ii) the STZ group, in which rats received an intraperitoneal injection of streptozotocin; (A) Representative micrographs of H&E-stained kidney sections and Periodic acid-Schiff-stained kidney sections from different groups. (B) Representative images of ultrastructure of glomeruli by transmission electron microscopy from different groups. Foot process is indicated by arrows.

Mitochondrial dysfunction and reduced sesn2 expression in podocytes from rats with STZ-induced diabetes. Even though mitochondrial dysfunction has been recognized as a crucial mediator of DKD, *in vivo* studies on podocyte mitochondria under HG conditions are limited, at least to the best of our knowledge. Given that the intact structure of the mitochondria

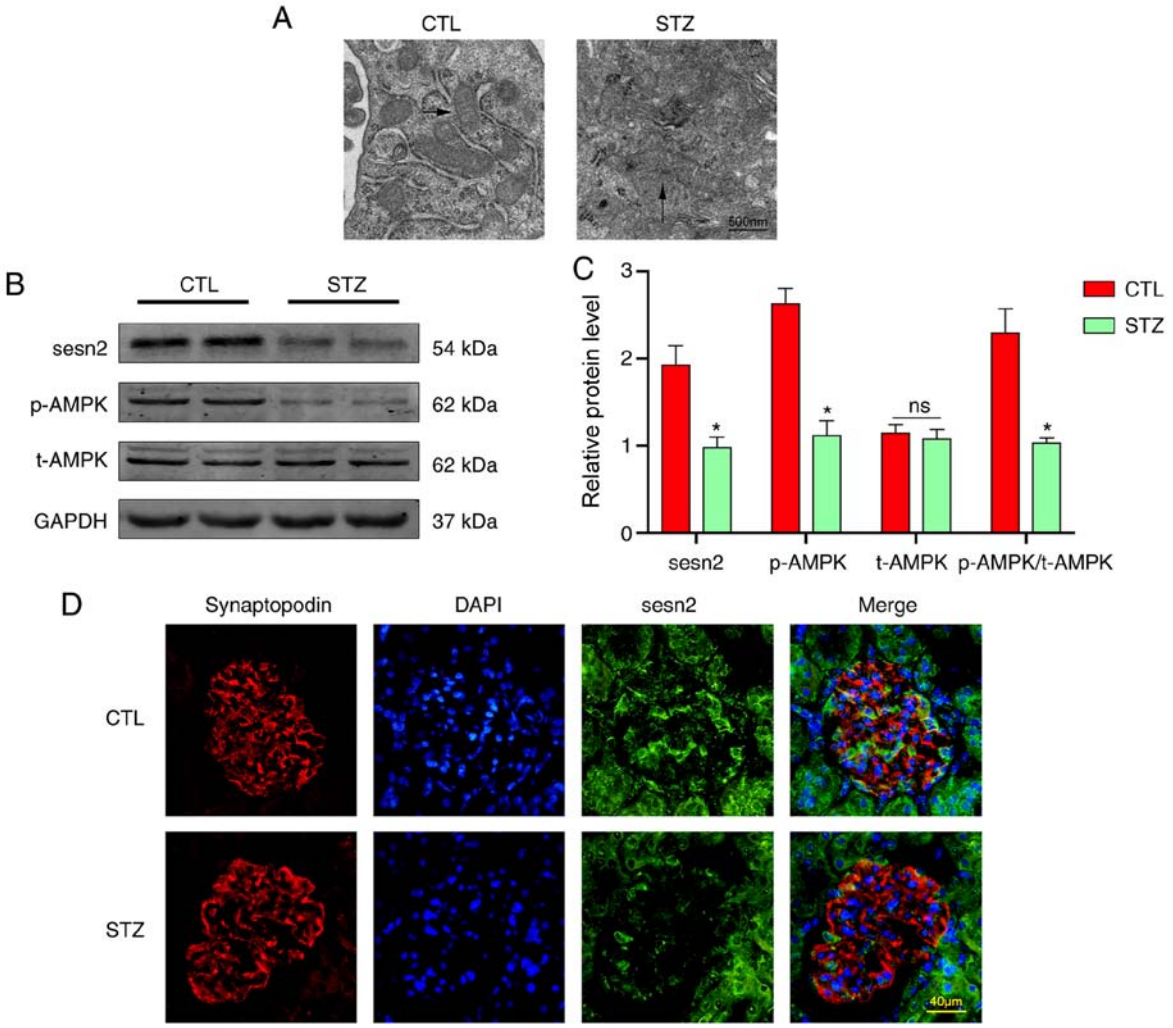

Figure 3. Mitochondrial dysfunction and reduced sesn2 expression in podocytes from streptozotocin-induced diabetic rats. Rats were divided into two groups: i) the control (CTL), where the rats received citrate buffer alone; and ii) the STZ group, where rats received an intraperitoneal injection of streptozotocin; (A) Representative images of ultrastructure of podocyte mitochondria (indicated by arrows) by transmission electron microscopy from different groups. (B and C) Representative western blots of glomerular sesn2, p-AMPK and AMPK expression and quantification in the different groups (*P<0.05 vs. CTL, n=6); (D) Representative images of immunofluorescent staining of synaptopodin, sesn2 and DAPI in the kidney sections from different groups. sesn2, sestrin-2; STZ, streptozotocin; AMPK, AMP-activated protein kinase.

represents a healthy organelle, the morphological changes in the mitochondria were the focus in the present study. Transmission electron microscopy revealed mitochondrial abnormalities, such as swelling and disorganization of the cristae in the rats with diabetes (Fig. 3A), which indirectly indicate impaired mitochondrial function.

To clarify the underlying mechanism of perturbed mitochondrial function, the expression of sesn2 was further evaluated, and was found to be decreased in the glomeruli of diabetic rats (Fig. 3B and D); this indicated that the HG-induced downregulation of sesn2 is associated with mitochondrial dysfunction.

AMPK is highly expressed in renal cells, such as podocytes, and plays a crucial role in maintaining glucose homeostasis (20). Previous studies have proposed a protective role for AMPK signaling in mitochondrial function (17,21,22). Notably, a decrease in the p-AMPK/AMPK protein ratio was witnessed in the diabetic rats, which prompted the investigation into the underlying role of sesn2 in AMPK regulation (Fig. 3B).

Changes in sesn2 and AMPK expression in cultured podocytes under HG conditions. To examine the effect of HG on sesn2 *in vitro*, human podocytes were treated with various concentrations of D-glucose (5, 15, 25 and 35 mM) for 24 h, and at different time points (0, 6, 12, 18 and 24 h) under HG conditions (35 mM). HG (35 mM) significantly decreased the sesn2 expression levels following 24 h of stimulation (Fig. 4A-D). Moreover, immunofluorescence assays revealed decreased sesn2 fluorescence in the cytoplasm of the HG-treated podocytes (Fig. 4H). To exclude the effects of D-mannitol on sesn2 expression in human podocytes, the results were compared with those of cells under normal culture conditions (Fig. 4E). Consistent with the results of the *in vivo* experiments, the HG-treated podocytes presented a decrease in the p-AMPK/AMPK protein ratio. Collectively, these results suggest that HG alters the expression of sesn2 and the phosphorylation of AMPK (Thr172) in podocytes.

Effects of HG on mitochondrial dysfunction in cultured podocytes. To further explore the potential mechanisms

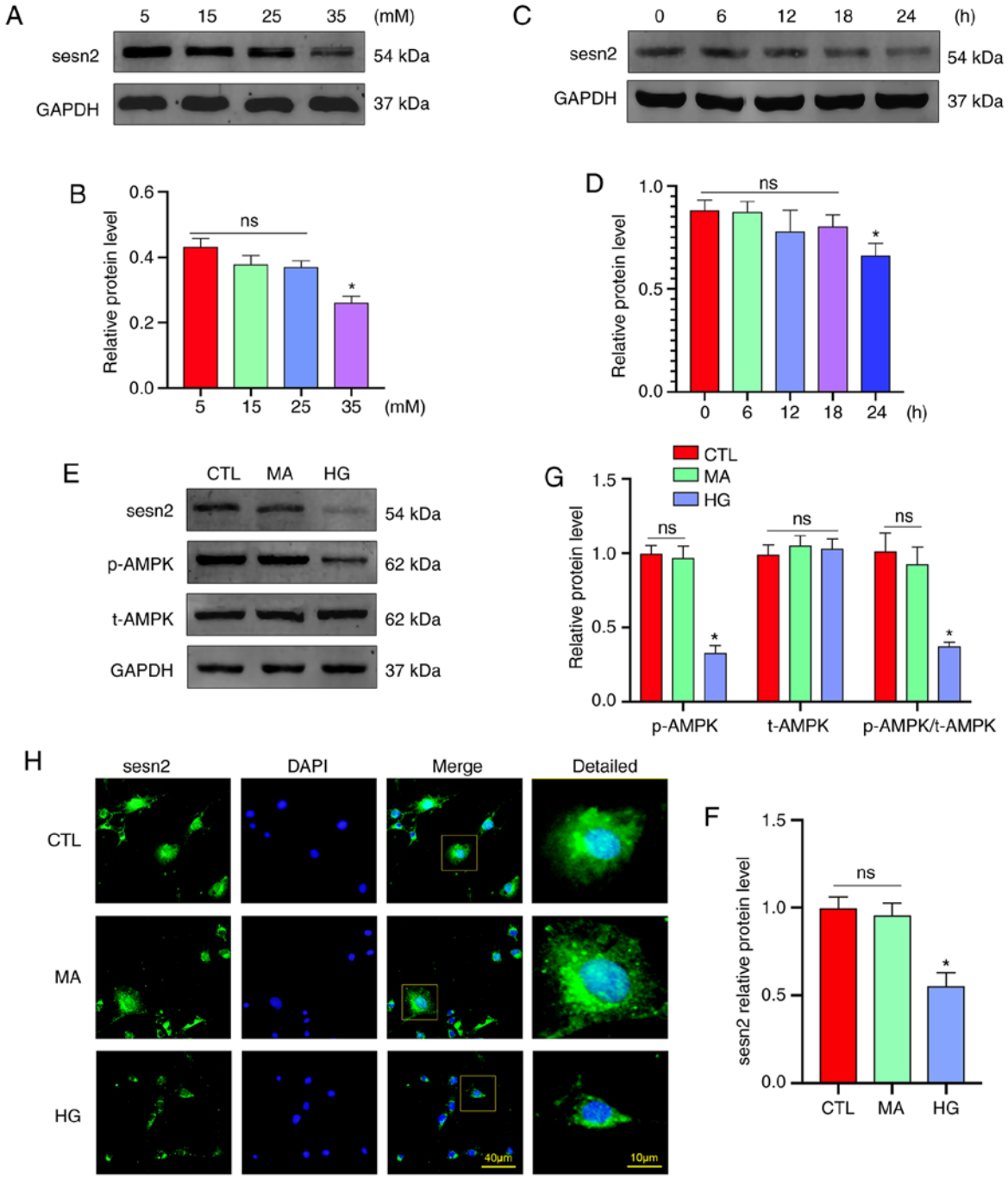

Figure 4. Changes in sesn2 and AMPK expression in cultured podocytes under HG conditions. (A and B) Representative western blots of sesn2 expression in cultured podocytes stimulated with various concentrations of glucose for 24 h and quantification of the results (*P<0.05 vs. 5 mM, n=3). (C and D) Representative western blots of sesn2 expression in cultured podocytes in 35 mM HG-treated podocytes at various time points and quantitation of the results (*P<0.05 vs. 0 h, n=3). (E-G) Representative western blots of sesn2, p-AMPK and AMPK expression and quantification of the results in podocytes cultured with different medium (*P<0.05 vs. CTL, n=3). (H) Immunofluorescence results of sesn2 in cultured podocytes in each group. Cells in the boxed area were magnified to show further details (show in 'Detailed' image on the right). CTL, 5 mM glucose for 24 h; MA, 5 mM glucose + 30 mM mannitol for 24 h; HG, 35 mM glucose for 24 h. sesn2, sestrin-2; AMPK, AMP-activated protein kinase; HG, high glucose; ns, not significant.

of podocyte apoptosis and mitochondrial dysfunction, the effects of HG were investigated *in vitro*. As shown in Fig. 5A and B, podocyte apoptosis was markedly increased under HG conditions. Subsequently, mitochondrial dysfunction was evaluated from several aspects. Firstly, transmission electron microscopy photomicrographs indicated severe mitochondrial swelling, cristae loss and a decreased matrix density in podocytes treated with HG (Fig. 5C), which were similar to the alterations observed in diabetic rats. Considering that the mitochondria are the primary producers of ROS (23), DCFH-DA (a fluorescent probe) was used to detect cellular oxidative stress, and it was revealed that intracellular ROS production was markedly increased in the podocytes under HG conditions (Fig. 5D). To a certain extent, MMP is an indicator of mitochondrial function; thus, JC-1 staining was used to reveal that HG exposure reduced MMP (Fig. 5F). Collectively, these results suggest that HG stimulation negatively affects the mitochondria and reduces

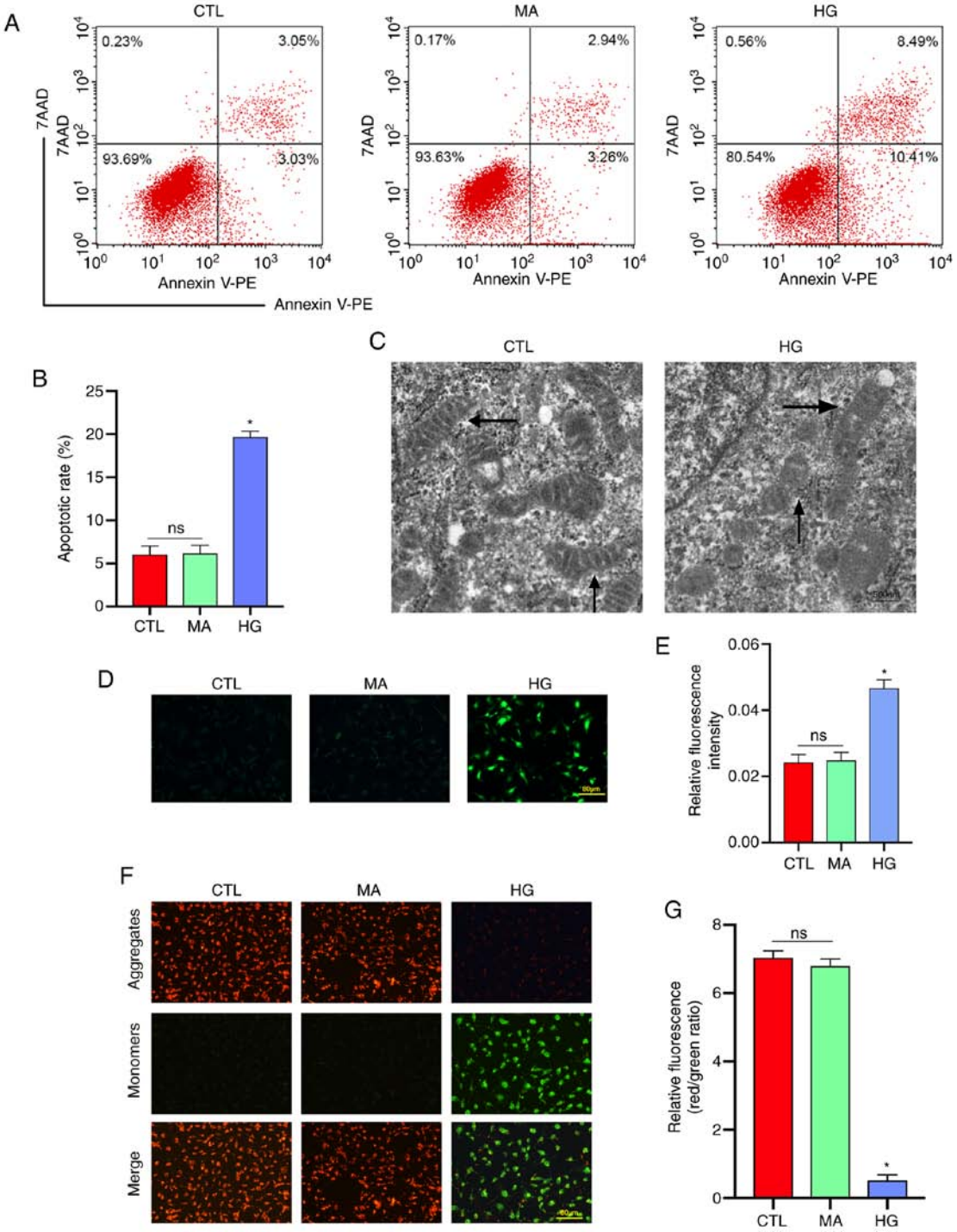

Figure 5. Effects of HG on mitochondrial dysfunction in cultured podocytes. Cells were divided into 3 groups: i) the control (CTL), where cells were cultured in 5 mM glucose for 24 h; ii) the MA group, where cells were cultured in 5 mM glucose and 30 mM mannitol for 24 h; iii) the HG group, where cells were cultured in 35 mM glucose for 24 h. (A and B) Flow cytometric analysis of apoptosis in cultured podocytes in different groups and quantification of the results (*P<0.05 vs. CTL, n=3). (C) Representative images of ultrastructure of cultured podocyte mitochondria (indicated by arrows) by transmission electron microscopy in different groups. (D and E) Representative images of ROS production in cultured podocytes in different groups. ROS production was assessed by the detection of DCFH-DA fluorescence (green) (*P<0.05 vs. CTL, n=3). (F and G) Representative images of mitochondrial membrane potential in podocytes by JC-1 staining in different groups and quantification of the results (*P<0.05 vs. CTL, n=3). sesn2, sestrin-2; AMPK, AMP-activated protein kinase; HG, high glucose; ns, not significant.

the sesn2 and p-AMPK levels, providing direct evidence that sesn2/AMPK signaling may play a significant role in the regulatory mechanism of mitochondrial dysfunction in podocytes.

Role of sesn2 in apoptosis and mitochondrial dysfunction in podocytes under HG conditions, via AMPK. To further examine the mechanisms through which sesn2 is involved in the regulation of AMPK and mitochondrial dysfunction, pc-DNA3.1-sesn2 plasmid and siRNA sesn2 were transfected into cultured podocytes. The transfection of pc-DNA3.1-sesn2 plasmid reversed the downregulation of sesn2 and the dephosphorylation of AMPK under HG conditions, while siRNA sesn2 decreased the phosphorylation of AMPK under normal

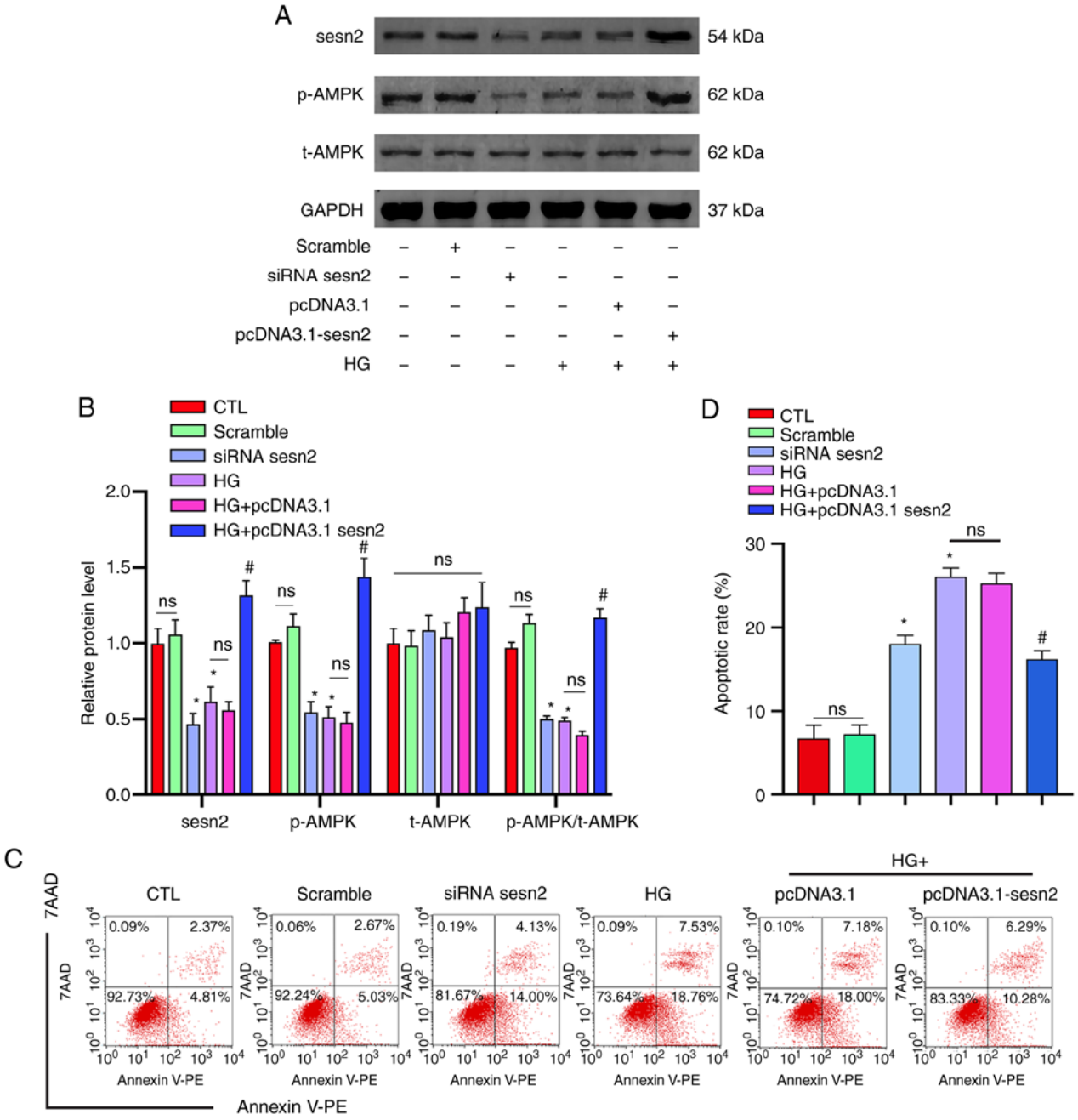

Figure 6. Role of sesn2 in apoptosis and mitochondrial dysfunction in podocytes under HG conditions through AMPK. Cells were divided into 6 groups: i) the control (CTL), where cells were cultured in 5 mM glucose for 24 h; ii) scramble, where cells were transfected with scramble siRNA and HiPerFect transfection reagent under normal conditions for 24 h; iii) siRNA sesn2, where cells were transfected with 6 nM sesn2 siRNA and HiPerFect transfection reagent under normal conditions for 24 h; iv) HG, where cells were cultured in 35 mM glucose for 24 h; v) HG + pcDNA3.1, where cells were transfected with negative control with pcDNA3.1 and the X-tremeGENETM Transfection Reagent under the 35 mM glucose condition for 24 h; vi) HG + pcDNA3.1 sesn2, cells were transfected with sesn2 plasmid and the X-tremeGENETM Transfection Reagent under the 35 mM glucose condition for 24 h. (A and B) Western blots to measure the protein levels of sesn2, p-AMPK and AMPK in cultured podocytes transfected with siRNA sesn2, siRNA-scrambles, pcDNA3.1-sesn2 or pcDNA3.1 (*P<0.05 vs. CTL, $^{\#}$P<0.05 vs. HG, n=3). (C and D) Flow cytometric analysis of apoptosis in cultured podocytes in different groups and quantification of the results (*P<0.05 vs. CTL, $^{\#}$P<0.05 vs. HG, n=3).

conditions (Fig. 6A and B), indicating that sesn2 positively regulates p-AMPK. Concurrently, sesn2 overexpression suppressed HG-induced apoptosis and mitochondrial defects in podocytes; by contrast, these phenomena were exacerbated by sesn2 knockdown (Fig. 6C-G). The results of immunoprecipitation indicated that sesn2 interacts with and regulates AMPK (Fig. 7I). Thus, these data confirm that the protective role of sesn2 in mitochondria and podocytes is the result of AMPK regulation (Fig. 8).

Role of AMPK in apoptosis and mitochondrial dysfunction in podocytes under HG conditions. To clarify the function of AMPK in podocytes, the AMPK activator, AICAR, and the inhibitor, C.C, were applied. The results revealed that treatment with AICAR under HG conditions restored AMPK phosphorylation, while C.C exacerbated the HG-induced decrease in AMPK phosphorylation (Fig. 7A and B). Additionally, AICAR decreased HG-induced apoptosis and mitochondrial dysfunction. On the contrary, C.C exacerbated

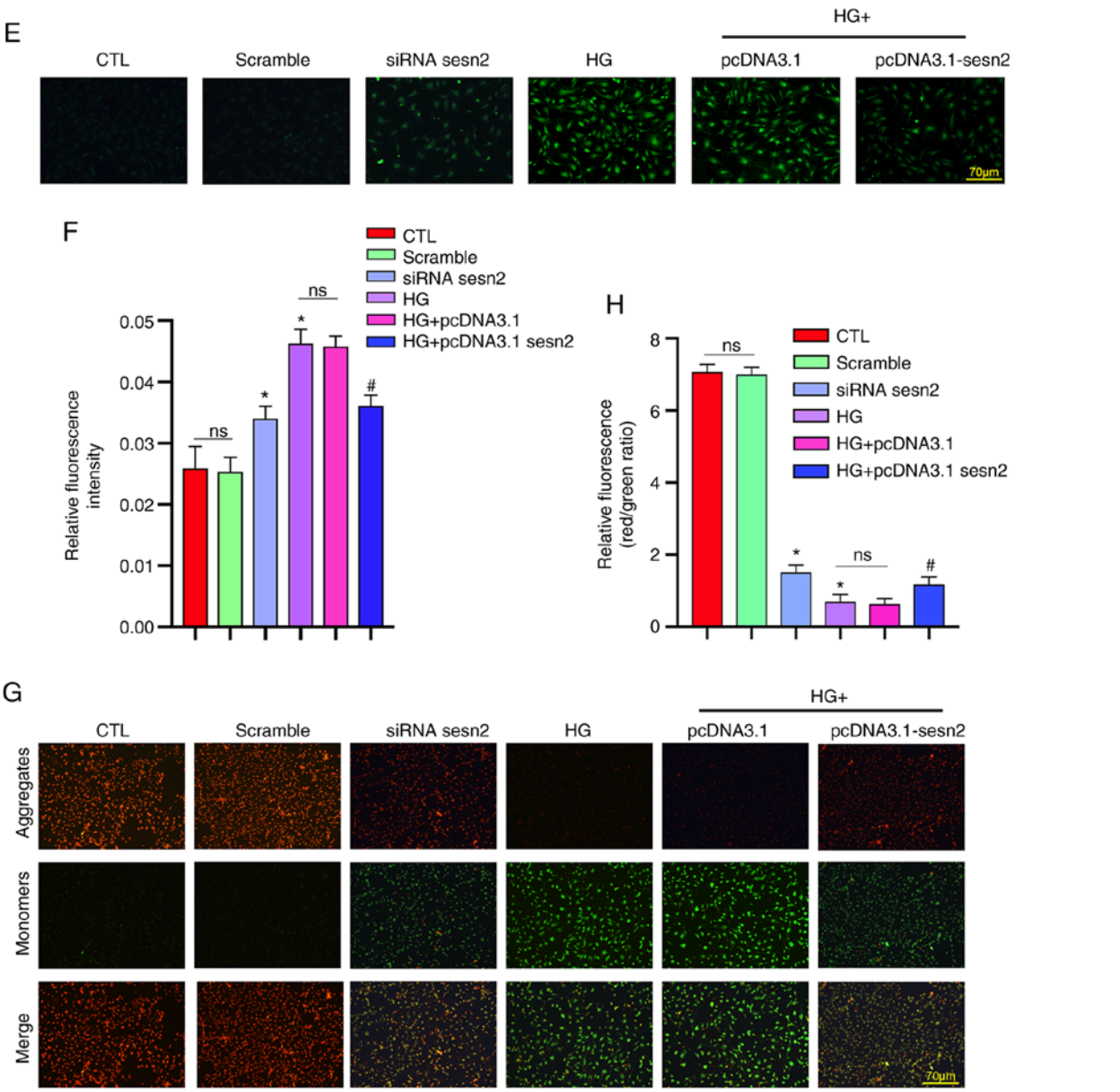

Figure 6. Continued. (E and F) Representative images of ROS production in cultured podocytes in different groups. ROS production was assessed by the detection of DCFH-DA fluorescence (green) (*P<0.05 vs. CTL, $^{\#}$P<0.05 vs. HG, n=3). (G and H) Representative images of mitochondrial membrane potential in podocytes by JC-1 staining in different groups and quantification of the results (*P<0.05 vs. CTL, $^{\#}$P<0.05 vs. HG, n=3). sesn2, sestrin-2; AMPK, AMP-activated protein kinase; HG, high glucose; ns, not significant.

podocyte apoptosis and mitochondrial dysfunction compared with the HG-only group (Fig. 7C-H). Taken together, these results demonstrated that AMPK exerts a protective effect on podocytes and mitochondria under HG conditions.

Discussion

Mitochondrial dysfunction has been implicated in podocyte injury and in the subsequent development of DKD (4,5); however, the key molecules involved in this mechanism have yet to be elucidated. The current study revealed that the expression of the stress-inducible protein, sesn2, was decreased in HG-stimulated podocytes, as well as those in diabetic rats and patients with DKD. Sesn2 also ameliorated the apoptosis and function of mitochondria in podocytes through AMPK signaling.

As a component of the glomerular filtration barrier, podocyte apoptosis contributes to the pathogenesis of DKD (24,25). Consistent with previous findings (26), the level of podocyte apoptosis was elevated under HG conditions in the present study (Fig. 5A and B). There are three primary mechanisms that regulate apoptosis, namely the mitochondrial, death receptor and endoplasmic reticulum pathways (27). Since mitochondrial dysfunction has been implicated in the pathogenesis of DKD (28), mitochondrial morphology was observed in diabetic rats. The results indicated mitochondrial abnormalities, including swelling, disorganization of the cristae or a loss of the cristae membrane (Fig. 3A), which resembles the phenotype of podocytes under HG (Fig. 5C). While swelling under HG stimulation, the mitochondrial permeability transition pore complex opens into the inner mitochondrial membrane, which enables free transit of molecules <1.5 KDa (including protons) into the

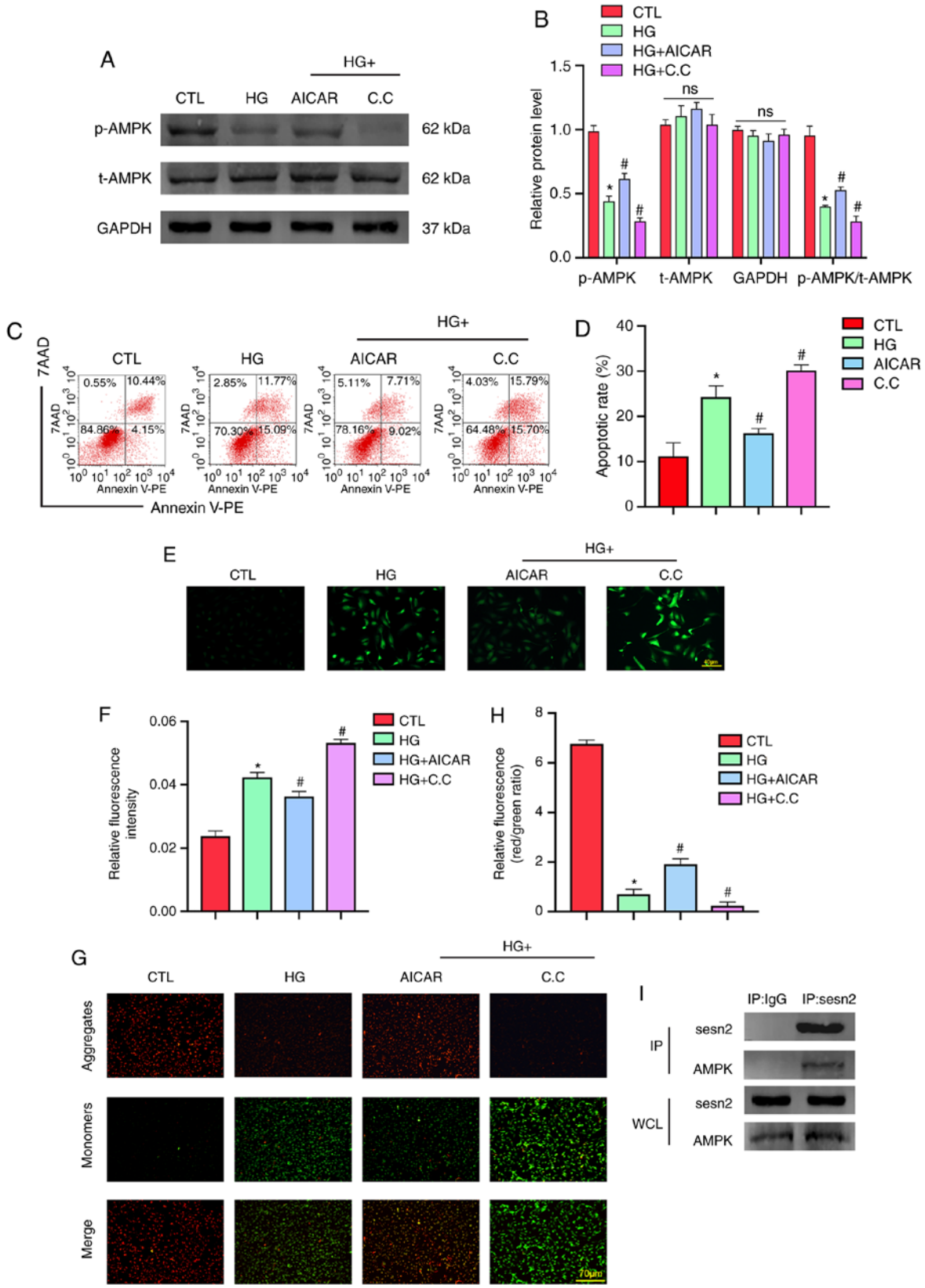

Figure 7. Role of AMPK in apoptosis and mitochondrial dysfunction in podocytes under HG. Cells were divided into 4 groups: i) the control (CTL), where cells were cultured in 5 mM glucose for 24 h; ii) HG, where cells were cultured in 35 mM glucose for 24 h; iii) HG + AICAR, where cells were cultured in 35 mM glucose in the presence of 1 mM AICAR for 24 h; iv) HG + compound C, where cells were cultured in 35 mM glucose for 24 h in the presence of 5 μM compound C for 2 h. (A and B) Western blots to measure the protein levels of p-AMPK and AMPK in cultured podocytes in different groups and quantification of the results (*P<0.05 vs. CTL, $^{\#}$P<0.05 vs. HG, n=3). (C and D) Flow cytometric analysis of apoptosis in cultured podocytes in different groups and quantification of the results (*P<0.05 vs. CTL, $^{\#}$P<0.05 vs. HG, n=3). (E and F) Representative images of ROS production in cultured podocytes in different groups. ROS production was assessed by detection of DCFH-DA fluorescence (green) (*P<0.05 vs. CTL, $^{\#}$P<0.05 vs. HG, n=3). (G and H) Representative images of mitochondrial membrane potential in podocytes by JC-1 staining in different groups and quantification of the results (*P<0.05 vs. CTL, $^{\#}$P<0.05 vs. HG, n=3). (I) Reciprocal immunoprecipitation of sesn2 and AMPK. Podocytes lysates were subject to immunoprecipitation with sesn2 antibody. The immunoprecipitates were then blotted with anti-AMPKα antibody. sesn2, sestrin-2; AMPK, AMP-activated protein kinase; HG, high glucose; ns, not significant.

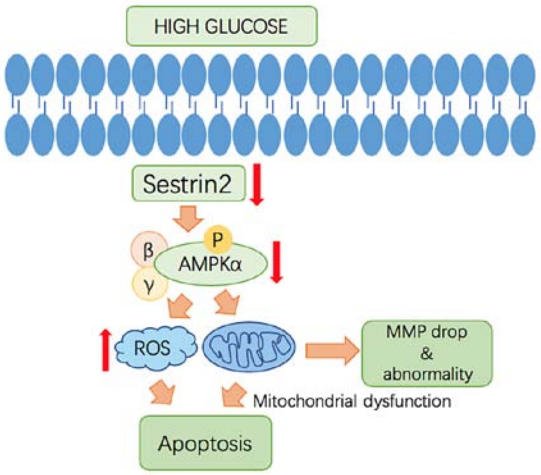

Figure 8. Schematic diagram of the mechanism of sestrin2 in mitochondrial dysfunction and apoptosis under HG conditions. sesn2, sestrin-2; AMPK, AMP-activated protein kinase; HG, high glucose; ns, not significant.

mitochondria. As a result, oxidative phosphorylation is disrupted and ATP is depleted (29). Subsequently, pro-apoptotic proteins, such as cytochrome *c* and apoptosis-inducing factor are released into the cytosol as a result of increased outer mitochondrial membrane permeabilization (MOMP) (30). Ultimately, these changes induce cell death via caspase-dependent and -independent pathways. Additionally, MMP was found to be decreased under HG stimulation in this study (Fig. 5F and G). As MMP plays a pivotal role in ATP generation, this decrease aligns with the disruption of mitochondrial homeostasis and the subsequent release of ROS into the cytosol (31). Therefore, in the present study, the levels of ROS were found to be elevated in podocytes under HG conditions (Fig. 5D and E), accounting for the upregulation of mitochondrial ROS production. Ultimately, the present study demonstrated that apoptosis was elevated in podocytes in a HG environment (Fig. 5A and B), which was at least partly due to the morphological disorder and malfunction of mitochondria (such as ROS accumulation and a decrease in MMP).

As a stress-inducible metabolic regulator, sesn2 has been proven to protect the mitochondria from oxidative damage both *in vivo* and *in vitro* (32,33). To clarify the potential association between sesn2 and AMPK, the expression of these two molecules was determined in diabetic rats (Fig. 3B-D), as well as in HG-cultured podocytes (Fig. 4A-H), revealing a decrease in both cases. Moreover, the decrease in sesn2 and p-AMPK was accompanied by reduced mitochondrial function (Fig. 5B-D); thus, sesn2/AMPK was postulated to preserve mitochondrial performance in podocytes. In order to verify this hypothesis, podocytes were transfected with a sesn2 expression plasmid prior to treatment with HG. The results suggested that sesn2 overexpression ameliorated podocyte apoptosis and increased AMPK phosphorylation (Fig. 6A-D). Cellular ROS production was also reduced when sesn2 was upregulated (Fig. 6E and F), which revealed that sesn2 reduced oxidative stress. At the same time, the decrease in MMP was alleviated by sesn2 overexpression (Fig. 6G and H), illustrating that sesn2 may stabilize the mitochondrial membrane. By contrast, sesn2 downregulation may be detrimental to both podocytes and mitochondria (Fig. 6C-G). The results also revealed that the activation of AMPK (using AICAR) was beneficial to podocytes under HG conditions, while AMPK inhibition (with C.C) was detrimental (Fig. 7C-H).

Sesn2 has been verified to directly bind and function upstream of AMPK (7,10,34,35), which was also confirmed in the present study (Fig. 7I). As a highly-conserved master regulator of metabolism, AMPK maintains metabolic homeostasis under metabolic stress conditions, both at the cellular and the physiological level. AMPK can sense cellular energy potential by directly binding to adenine nucleotides. Following alterations in available energy and subsequent changes in the ADP/ATP ratio, activated AMPK redirects metabolism towards increased catabolic processes, as well as decreased anabolism, via the phosphorylation of key proteins involved in mitochondrial homeostasis (36-39), including receptor γ coactivator-1α (40,41).

In conclusion, the findings of the present study demonstrates that sesn2 may alleviate podocyte apoptosis under HG conditions, which may be attributed to the protection of the mitochondria via AMPK activation, including reduced ROS production, MMP stabilization and maintaining mitochondrial morphology (Fig. 8). Further studies are required to determine whether other mechanisms are involved in this process through which sesn2 regulates AMPK, and whether other downstream molecules are involved in the protection of podocyte mitochondria.

Acknowledgements

Not applicable.

Funding

The present study was supported by the National Science Foundation of China (grant. no. 81770687 to GD and no. 81800615 to YM).

Availability of data and materials

The materials described in the manuscript, including all relevant raw data, are freely available from the corresponding author to any scientist wishing to use them for non-commercial purposes, without breaching participant confidentiality.

Authors' contributions

QL and GD conceived and designed the experiments. QL, YM, ZC, JH, YF, CC and WL performed the experiments. QL analyzed the data, drafted and critically revised the manuscript. GD read and revised the final version of the manuscript. All authors have read and approved the final manuscript.

Ethics approval and consent to participate

Experiments were performed according to the approved guidelines of Wuhan University and were approved by the Research Ethics Committee of Renmin Hospital of Wuhan University after written informed consent was received from the patients. All animal experiments conformed to the Regulations of Animal Experiments in Wuhan University, and were approved by the Ethics Committee for the Experimental Use of Animals at Renmin Hospital of Wuhan University.

Patient consent for publication

Not applicable.

Competing interests

The authors declare that they have no competing interests.

References

1. Locatelli F, Pozzoni P and Del Vecchio L: Renal replacement therapy in patients with diabetes and end-stage renal disease. J Am Soc Nephrol 15 (Suppl 1): S25-S29, 2004.
2. Szrejder M and Piwkowska A: AMPK signalling: Implications for podocyte biology in diabetic nephropathy. Biol Cell 111: 109-120, 2019.
3. Jefferson JA, Alpers CE and Shankland SJ: Podocyte biology for the bedside. Am J Kidney Dis 58: 835-845, 2011.
4. Higgins GC and Coughlan MT: Mitochondrial dysfunction and mitophagy: The beginning and end to diabetic nephropathy? Br J Pharmacol 171: 1917-1942, 2014.
5. Yuan Y, Huang S, Wang W, Wang Y, Zhang P, Zhu C, Ding G, Liu B, Yang T and Zhang A: Activation of peroxisome proliferator-activated receptor-γ coactivator 1α ameliorates mitochondrial dysfunction and protects podocytes from aldosterone-induced injury. Kidney Int 82: 771-789, 2012.
6. Granata S, Dalla Gassa A, Tomei P, Lupo A and Zaza G: Mitochondria: A new therapeutic target in chronic kidney disease. Nutr Metab (Lond) 12: 49, 2015.
7. Budanov AV, Lee JH and Karin M: Stressin' Sestrins take an aging fight. EMBO Mol Med 2: 388-400, 2010.
8. Lee JH, Budanov AV and Karin M: Sestrins orchestrate cellular metabolism to attenuate aging. Cell Metab 18: 792-801, 2013.
9. Budanov AV, Sablina AA, Feinstein E, Koonin EV and Chumakov PM: Regeneration of peroxiredoxins by p53-regulated sestrins, homologs of bacterial AhpD. Science 304: 596-600, 2004.
10. Budanov AV and Karin M: p53 target genes sestrin1 and sestrin2 connect genotoxic stress and mTOR signaling. Cell 134: 451-460, 2008.
11. Lee JH, Budanov AV, Park EJ, Birse R, Kim TE, Perkins GA, Ocorr K, Ellisman MH, Bodmer R, Bier E and Karin M: Sestrin as a feedback inhibitor of TOR that prevents age-related pathologies. Science 327: 1223-1228, 2010.
12. Woo HA, Bae SH, Park S and Rhee SG: Sestrin 2 is not a reductase for cysteine sulfinic acid of peroxiredoxins. Antioxid Redox Signal 11: 739-745, 2009.
13. Bae SH, Sung SH, Oh SY, Lim JM, Lee SK, Park YN, Lee HE, Kang D and Rhee SG: Sestrins activate Nrf2 by promoting p62-dependent autophagic degradation of Keap1 and prevent oxidative liver damage. Cell Metab 17: 73-84, 2013.
14. Budanov AV, Shoshani T, Faerman A, Zelin E, Kamer I, Kalinski H, Gorodin S, Fishman A, Chajut A, Einat P, *et al*: Identification of a novel stress-responsive gene Hi95 involved in regulation of cell viability. Oncogene 21: 6017-6031, 2002.
15. Maiuri MC, Malik SA, Morselli E, Kepp O, Criollo A, Mouchel PL, Carnuccio R and Kroemer G: Stimulation of autophagy by the p53 target gene Sestrin2. Cell Cycle 8: 1571-1576, 2009.
16. Lee JH, Budanov AV, Talukdar S, Park EJ, Park HL, Park HW, Bandyopadhyay G, Li N, Aghajan M, Jang I, *et al*: Maintenance of metabolic homeostasis by Sestrin2 and Sestrin3. Cell Metab 16: 311-321, 2012.
17. Dugan LL, You YH, Ali SS, Diamond-Stanic M, Miyamoto S, DeCleves AE, Andreyev A, Quach T, Ly S, Shekhtman G, *et al*: AMPK dysregulation promotes diabetes-related reduction of superoxide and mitochondrial function. J Clin Invest 123: 4888-4899, 2013.
18. Shrestha B and Dunn L: The declaration of helsinki on medical research involving human subjects: A review of seventh revision. J Nepal Health Res Conc 17: 548-552, 2020.
19. Hu J, Yang Q, Chen Z, Liang W, Feng J and Ding G: Small GTPase Arf6 regulates diabetes-induced cholesterol accumulation in podocytes. J Cell Physiol 234: 23559-23570, 2019.
20. Cammisotto PG and Bendayan M: Adiponectin stimulates phosphorylation of AMP-activated protein kinase alpha in renal glomeruli. J Mol Histol 39: 579-584, 2008.
21. Cai X, Bao L, Ren J, Li Y and Zhang Z: Grape seed procyanidin B2 protects podocytes from high glucose-induced mitochondrial dysfunction and apoptosis via the AMPK-SIRT1-PGC-1α axis in vitro. Food Funct 7: 805-815, 2016.
22. Madhavi YV, Gaikwad N, Yerra VG, Kalvala AK, Nanduri S and Kumar A: Targeting AMPK in diabetes and diabetic complications: Energy homeostasis, autophagy and mitochondrial health. Curr Med Chem 26: 5207-5229, 2019.
23. Ma Y and Li J: Metabolic shifts during aging and pathology. Compr Physiol 5: 667-686, 2015.
24. Butt A and Riaz S: Study of protein profiling of human urine in diabetic hypertensive nephropathy versus normal healthy controls. Diabetes Technol Ther 12: 379-386, 2010.
25. Piwkowska A, Rogacka D, Audzeyenka I, Jankowski M and Angielski S: High glucose concentration affects the oxidant-antioxidant balance in cultured mouse podocytes. J Cell Biochem 112: 1661-1672, 2011.
26. Ma Y, Yang Q, Chen X, Liang W, Ren Z and Ding G: c-Abl contributes to glucose-promoted apoptosis via p53 signaling pathway in podocytes. Diabetes Res Clin Pract 113: 171-178, 2016.
27. Redza-Dutordoir M and Averill-Bates DA: Activation of apoptosis signalling pathways by reactive oxygen species. Biochim Biophys Acta 1863: 2977-2992, 2016.
28. Galvan DL, Green NH and Danesh FR: The hallmarks of mitochondrial dysfunction in chronic kidney disease. Kidney Int 92: 1051-1057, 2017.
29. Halestrap AP: What is the mitochondrial permeability transition pore? J Mol Cell Cardiol 46: 821-831, 2009.
30. Orrenius S, Gogvadze V and Zhivotovsky B: Calcium and mitochondria in the regulation of cell death. Biochem Biophys Res Commun 460: 72-81, 2015.
31. Green DR and Reed JC: Mitochondria and apoptosis. Science 281: 1309-1312, 1998.
32. Quan N, Wang L, Chen X, Luckett C, Cates C, Rousselle T, Zheng Y and Li J: Sestrin2 prevents age-related intolerance to post myocardial infarction via AMPK/PGC-1α pathway. J Mol Cell Cardiol 115: 170-178, 2018.
33. Hwang HJ, Kim JW, Chung HS, Seo JA, Kim SG, Kim NH, Choi KM, Baik SH and Yoo HJ: Knockdown of Sestrin2 increases lipopolysaccharide-induced oxidative stress, apoptosis, and fibrotic reactions in H9c2 cells and heart tissues of Mice via an AMPK-dependent mechanism. Mediators Inflamm 2018: 6209140, 2018.
34. Kim HJ, Joe Y, Kim SK, Park SU, Park J, Chen Y, Kim J, Ryu J, Cho GJ, Surh YJ, *et al*: Carbon monoxide protects against hepatic steatosis in mice by inducing sestrin-2 via the PERK-eIF2α-ATF4 pathway. Free Radic Biol Med 110: 81-91, 2017.
35. Liu X, Niu Y, Yuan H, Huang J and Fu L: AMPK binds to Sestrins and mediates the effect of exercise to increase insulin-sensitivity through autophagy. Metabolism 64: 658-665, 2015.
36. Egan DF, Shackelford DB, Mihaylova MM, Gelino S, Kohnz RA, Mair W, Vasquez DS, Joshi A, Gwinn DM, Taylor R, *et al*: Phosphorylation of ULK1 (hATG1) by AMP-activated protein kinase connects energy sensing to mitophagy. Science 331: 456-461, 2011.
37. Toyama EQ, Herzig S, Courchet J, Lewis TL Jr, Losón OC, Hellberg K, Young NP, Chen H, Polleux F, Chan DC and Shaw RJ: Metabolism. AMP-activated protein kinase mediates mitochondrial fission in response to energy stress. Science 351: 275-281, 2016.
38. Zong H, Ren JM, Young LH, Pypaert M, Mu J, Birnbaum MJ and Shulman GI: AMP kinase is required for mitochondrial biogenesis in skeletal muscle in response to chronic energy deprivation. Proc Natl Acad Sci USA 99: 15983-15987, 2002.
39. Jager S, Handschin C, St-Pierre J and Spiegelman BM: AMP-activated protein kinase (AMPK) action in skeletal muscle via direct phosphorylation of PGC-1alpha. Proc Natl Acad Sci USA 104: 12017-12022, 2007.
40. Canto C and Auwerx J: PGC-1alpha, SIRT1 and AMPK, an energy sensing network that controls energy expenditure. Curr Opin Lipidol 20: 98-105, 2009.
41. Ventura-Clapier R, Garnier A and Veksler V: Transcriptional control of mitochondrial biogenesis: The central role of PGC-1alpha. Cardiovasc Res 79: 208-217, 2008.